UNSTEADY STALL OF AXIAL FLOW COMPRESSORS

Prepared for:

U. S. ARMY
HARRY DIAMOND LABORATORIES
WASHINGTON 25, D.C.

FIRST QUARTERLY PROGRESS REPORT

By: W. G. Brady

Contract No. DA-49-186-AM-13(X)
CAL Report No. AM-1762-A-1
March 1963

CORNELL AERONAUTICAL LABORATORY, INC.
OF CORNELL UNIVERSITY, BUFFALO 21, N. Y.

CORNELL AERONAUTICAL LABORATORY, INC.
BUFFALO 21, NEW YORK

CAL REPORT NO. AM-1762-A-1

UNSTEADY STALL OF AXIAL FLOW COMPRESSORS

CONTRACT NO. DA-49-186-AM-13(X)

MARCH 1963

Prepared for:
U. S. ARMY
HARRY DIAMOND LABORATORIES
WASHINGTON 25, D.C.

TABLE OF CONTENTS

LIST OF FIGURES

I SUMMARY

The work done during the first quarter on "Research on Unsteady Stall of Axial Flow Compressors", Contract No. DA-49-186-AM-13(X), for the Harry Diamond Laboratories, Washington, D. C., by Cornell Aeronautical Laboratory, Inc. is reported here.

Initial effort in this program is concentrated on continuation of previous research at CAL concerning (1) an experimental study of the separation of a laminar boundary layer from walls moving upstream and downstream in a steady flow using a shrouded rotating cylinder in a wind tunnel, and (2) an analytical study of compatibility conditions between circulation disturbances on an actuator disc in a mean flow with swirl and the appearance of vorticity downstream of the disc.

The rotating cylinder apparatus was assembled and checked out. Certain modifications to the equipment were made to obtain the performance required for accurate boundary-layer measurements. Pressure distributions have been obtained for both the unshrouded and shrouded rotating cylinder. Preliminary boundary-layer data were obtained with small static and total head probes.

The analysis completed during the previous research for a mean flow with free-vortex-type swirl through a single-stage compressor was reviewed, and an error in the basic differential equations discovered. It was determined that the error did not affect the results obtained. The differential equations for a similar case, but with wheel-type swirl, were set up. As yet, a solution has not been obtained for this case. Results were obtained for a simplified flow which is an approximation to the flow through a single-stage compressor in a narrow annulus. In this case, it was found that, within the limitations of the small perturbation theory used, the only possible propagating type of disturbance in circulation on the actuator disc is one fixed in and rotating with the blades.

II INTRODUCTION

Rotating stall has been a continuing problem for the designers of axial-flow turbojet engines since the inception of their use in aircraft. For the compressor designer, the major problem associated with rotating stall has been one of blade fatigue failure resulting from blade resonance with the passage of stall zones. From a performance point of view, unsteady stall phenomena may place severe limitations on the acceleration or deceleration of a jet engine.

Extensive research effort has been devoted to this problem during the past two decades. Progress was made in that a degree of understanding of the phenomenon was attained; however, the basic problem remained unsolved when lack of funds reflecting a declining interest in jet engine development brought this research effort nearly to a halt in the late 1950's. In particular, the unsteady boundary-layer separation phenomena which, presumably, underlie rotating stall of compressor elements continue to pose problems of fundamental interest.

Due to a revival of interest in axial-flow jet engine development, this program was initiated to continue a methodical approach to solutions for the problems posed by unsteady compressor stall. The work reported here is a continuation of a research program concerning rotating stall in axial-flow compressors, carried out by the Cornell Aeronautical Laboratory over a three-year period ending in January 1959. The present program is a research effort for the purpose of increasing understanding of rotating stall and other unsteady surge characteristics of axial compressors. Included in this effort will be studies of the aerodynamics of compressor stages, studies of unsteady sectional-lift characteristics of single-blade elements near stall, and studies of possible methods of alleviating unsteady surge characteristics. In the current year's effort, the initial emphasis is on the continuation of two studies started under the original program: (1) a theoretical study of the role of entering swirl pattern in causing rotating stall of a single stage, and (2) an experimental study of the separation criteria for a moving surface (shrouded rotating cylinder).

III WORK ACCOMPLISHED

A. Rotating Cylinder Experiments

This work is a continuation of the research reported in Reference 1. The experiments were motivated by the need to establish criteria for the conditions for separation in a quasi-steady laminar boundary layer in the case involving a moving separation point. The theoretical work leading up to the experimental program was reported in Reference 2.

During the previous work, it was found in analyzing the quasi-steady boundary layer near separation that the problem involving a moving separation point could be reduced to a steady-flow problem in which the wall is in motion. This problem was treated separately for the cases of the wall in downstream motion and in upstream motion. In the former case, Sketch A, it was found that vanishing shear occurred at some distance, proportional to wall velocity, upstream of separation, and separation was characterized by a separated region embedded in the flow.

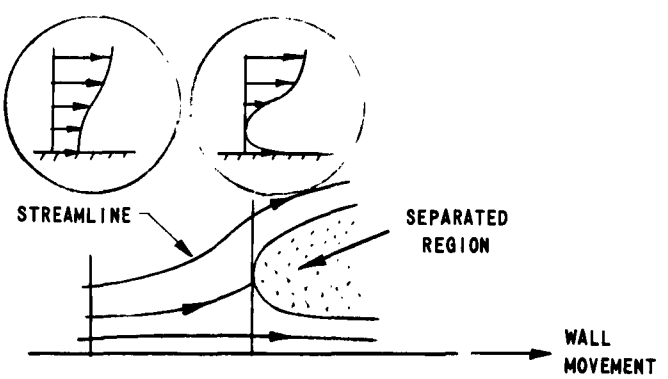

SKETCH A
WALL MOVING DOWNSTREAM

In this instance, separation would not occur at the wall, but at a finite height above the wall, and there would be a boundary-layer flow beneath the wake region. The analysis provides quantitative estimates of the displacement of the separation point due to wall velocity and of the position of the separation point above the wall. These results depend somewhat on the assumed velocity profile at separation, and are valid only for wall velocities which are small in comparison with the free-stream velocity. Accordingly, the experimental program was set up to determine the validity of the assumed profile, and to measure the effects of small and large wall velocities on the position of separation as a check on the theory.

In the case of the upstream moving wall, Sketch B, it was hypothesized that a probable profile at separation was one that flattened against the axis over a relatively large height with a singularity at the foot; that is, one in which the velocity abruptly changed from zero near the wall to the wall velocity at the wall.

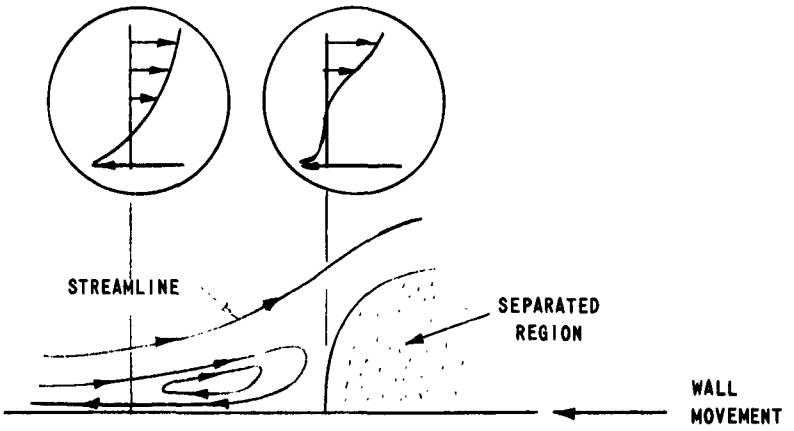

SKETCH B
WALL MOVING UPSTREAM

In this model, the boundary layer then contains a sublayer of circulating flow extending from the forward stagnation point to the separation point and, rigorously, there would be no wake flow into the boundary layer. The theory

indicates that, in this case, the separation point would be displaced upstream a distance proportional to the wall velocity, but provides no quantitative estimate of the displacement. It is noted that this result is somewhat speculative in that it is largely dependent on the assumed profile at separation. In order to clarify the upstream moving case, the experiments were designed to investigate the velocity profile near separation to assess the validity of the assumed singular profile. It was anticipated, of course, that a singular profile in the mathematical sense would not be observed and that there would be some flow from the wake into the boundary layer. If the height of this reverse flow were found to be small in comparison with the height over which the profile was flattened, then the assumed profile would be substantially verified. If this were not the case, the experimental profiles would serve as a basis for improving the analysis. Also, since the analysis provided no quantitative estimates of the displacement of the separation point due to wall velocity, the experiments were to provide this information.

Since the analysis demonstrated the equivalence of the quasi-steady problem and the problem of a moving wall at separation, the model chosen to experimentally investigate unsteady separation was a rotating cylinder in steady flow. This model simulates the pertinent features of the unsteady problem in that the wall and separation point are in relative motion, and both upstream and downstream moving walls are present. Of course, the chief feature of this experiment is that it is a steady-flow experiment, and more precise measurements are feasible. The method suffers somewhat in that a relatively steep pressure gradient is present at separation, and the effects of a moving wall on delaying or promoting separation might be difficult to evaluate if they were small in comparison with the effect of the strong pressure gradient. Also, because of the Magnus effect, the pressure distribution depends on the wall velocity, and observed shifts in separation might be the result of a change in pressure distribution. In order to circumvent these difficulties, provisions were made to shroud the model so that a more moderate airfoil-type pressure gradient could be imposed on the cylinder. This would not necessarily remove the Magnus effect, but it was anticipated that, by measuring the pressure distribution on the model as a function of rotation, it would be possible to change the shroud shape and maintain a given pressure distribution.

Experimental Apparatus

The basic apparatus is the equipment that was used for the previous investigation and consists of a 4-in. diameter cylinder mounted between plastic endplates, spanning the full width of the subsonic test section of the CAL One-Foot, High-Speed Wind Tunnel. The cylinder is mounted on bearings so as to rotate about its centerline.

The cylinder is instrumented with a piezoelectric pressure transducer vented through a 1/8-in. diameter hole in the surface of the cylinder. The usable frequency range of the pressure transducer and vent are 0 - 40, 000 cps; however, filters are incorporated in the recording system to limit response to the range between one cps and 1000 cps in order to eliminate steady-state and slowly changing centrifugal effects, and spurious electrical and acoustic noise. The output of the pressure transducer is displayed on a Tektronix Type 502 Oscilloscope and is recorded photographically. Rotation speeds of the cylinder are measured by means of a miniature electromagnetic pickup in conjunction with a 60-tooth gear attached to the cylinder shaft. The output of the pickup is displayed on the oscilloscope as well as on a Berkeley Counter and Timer.

A substantial portion of the work of this first quarter has been devoted to reassembly and checkout of the apparatus. Preliminary tests of the rotating cylinder showed that the performance of the Onsrud Air Turbine cylinder drive motor would be unsatisfactory for boundary layer survey work, where constant rpm must be held closely for extended lengths of time. The rotational speeds varied continuously over a wide range. Furthermore, fine control of rpm was extremely difficult. Therefore, the air turbine was replaced by a Heller Electrical Motor and Controller Unit, Model 2T60. Subsequent tests have shown that drift of this unit is very small, and fine control is possible. Rotational speed variations can be kept within $\pm$ 1% without difficulty.

Also during the preliminary shakedown tests, it was found that the cylinder driveshaft was bent slightly. This caused excessive vibration and runout, or eccentricity, of the cylinder. A new driveshaft was fabricated, and

one of the bearings replaced. Subsequent tests showed that the vibration had been reduced to a satisfactory level. Also, runout of the cylinder surface is now a maximum of 0.0003 in., which is quite satisfactory.

Shrouds were available from the previous program, as noted above. These shrouds are mounted above and below the cylinder and were designed so as to impose a more gradual, airfoil-type pressure gradient than exists on the unshrouded cylinder.

It is intended that the bulk of the boundary layer velocity survey work will be done with hot-wire anemometer equipment. This type of velocity probe is required, rather than the conventional total pressure probe, because the essential boundary layer velocity data must be obtained in the approximately 0.01 in. layer immediately adjacent to the cylinder. However, small diameter total head and static probes have been adapted to the traversing mechanism* and are also being used in the boundary layer investigations. The total head probe is particularly useful in defining the outer edge of the boundary layer. The flow velocity outside the boundary layer may vary continuously with distance away from the cylinder surface, but the total pressure approaches a constant value as the outer edge of the boundary layer is reached.

Details of the CAL One-Foot, High-Speed Wind Tunnel are presented in References 1 and 3. The configuration of the wind tunnel being used in the current tests are as described in Reference 1; stream turbulence level, and test section calibrations indicated in Reference 1 should be applicable to the present work.

Complete details of the experimental apparatus are included in Reference 1. Those minor modifications which have been incorporated during the present program have been noted above.

---

* The traversing mechanism is a jeweler's lathe slide-rest, or compound, mounted on top of the wind tunnel test section. Slots cut in the top of the test section and in the top shroud permit the probes to be used in the proximity of the cylinder surface.

Experimental Data Obtained to Date

Figure 1 illustrates the notation used for the rotating cylinder experiments. With the free-stream velocity as shown, cylinder angular rotation velocity is positive counterclockwise; the angle on the cylinder is measured from the horizontal reference (radius parallel to free-stream direction), positive in a counterclockwise direction; angles between 0° and $+180^{\circ}$ are on the upper surface of the cylinder, and between 0° and -180° on the lower surface. In the boundary layer, y is the distance away from the surface of the cylinder along the local normal to the surface, V is the peripheral speed of the surface of the cylinder, and v_b is the local velocity in the boundary layer parallel to the tangent plane to the cylinder surface. U is the free-stream velocity.

Pressure distributions have been obtained for the unshrouded rotating cylinder at various rpm's. These data are essentially in agreement with corresponding data presented in Reference 1. The unsteady pressure fluctuations noted in Reference 1 for the unshrouded rotating cylinder, attributed to vortex shedding, were also obtained.

Pressure distributions for the shrouded rotating cylinder have been obtained over a range of positive and negative rpm. This type of data had not been obtained during the previous work. Figure 2 shows a typical oscillograph record of traces from the output of the cylinder pressure transducer for Ω = -1284 rpm, U = 58.3 fps; this corresponds to a V / U of 0.385. Also shown in Figure 2 are the corresponding wind-off calibration traces. In both cases, the traces shown include at least five consecutive double cycles superimposed one on top of the other; hence, the results shown in Figure 2 are indicative of repeatability of the pressure data and, also, steadiness of the flow over the shrouded cylinder. Also apparent in the data of Figure 2 is a certain amount of contact noise, evidenced by the relatively high frequency uneveness in the traces. Note, in particular, the large "pip" in the middle of both sets of traces in Figure 2. The appearance of such contact noise in the traces has some consistency, but not enough to be accurately calibrated out. Therefore, when this data is reduced, a smooth faired curve is drawn through what appears to be the average of the traces recorded.

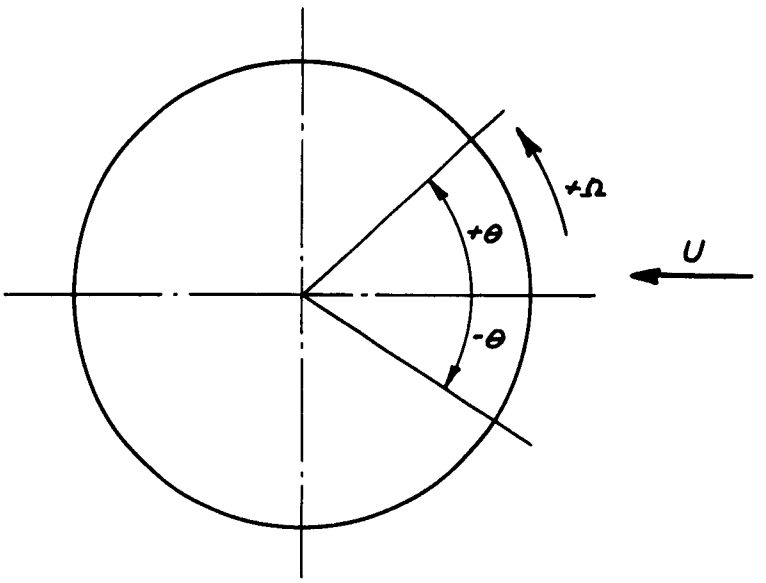

(a) ROTATING CYLINDER

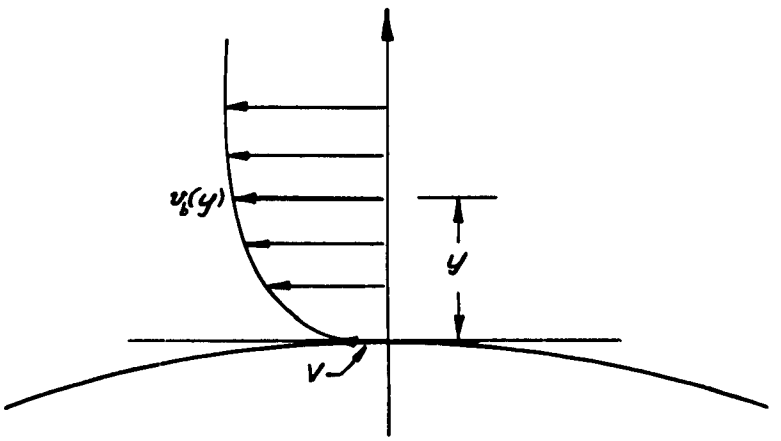

(b) BOUNDARY LAYER ON CYLINDER

Figure 1 NOTATION FOR ROTATING CYLINDER EXPERIMENTS

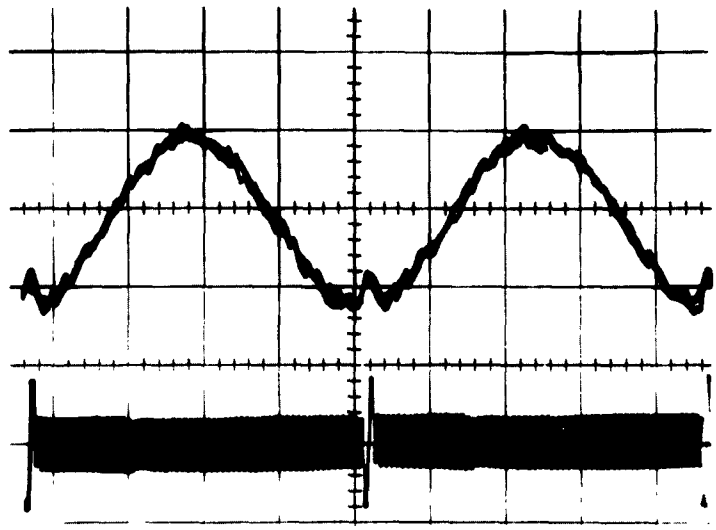

WIND-OFF CALIRATION
Ω = -1290 RPM

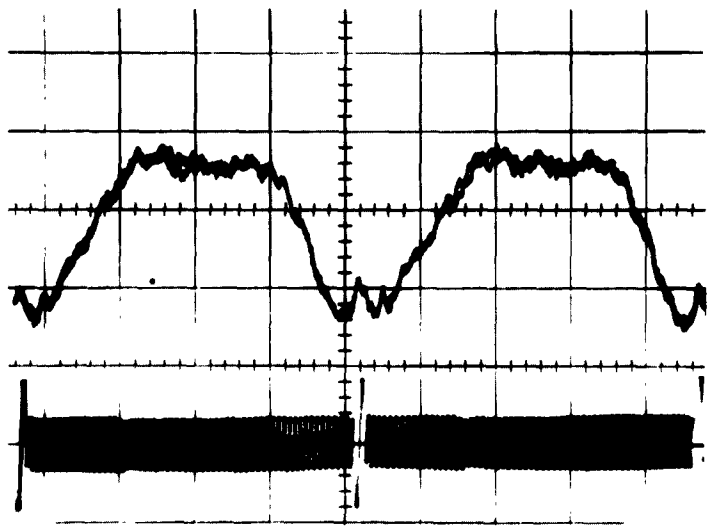

1815

U = 58.3 FPS, $(Re)_D$ = 1.2 x 10^5
Ω = -1284 RPM, V/U = 0.385

Figure 2 OSCILLOGRAPH RECORDS OF PRESSURE DISTRIBUTION ON ROTATING CYLINDER

Figure 3 shows the static pressure distribution in terms of the pressure coefficient for the same conditions as the Figure 2 data. Here, Δp_s is the difference between the local and the free-stream static pressures, and q is the free-stream dynamic pressure. The same technique is being used to reduce the oscillograph data as was used in Reference 1. The plotted data in Figure 3 was obtained from averages of at least five traces for two successive cycles in each trace. The differences between the two cycles of data are believed representative of scatter resulting primarily from the contact noise and the data reduction method which must be used; these data show the largest scatter obtained from the shrouded cylinder data thus far reduced. Figure 4 shows similar data for U = 58.3 fps, Ω = +712 rpm, where much better agreement between the time-averaged data for two cycles was obtained. Also shown on Figures 3 and 4 are static pressure coefficient data obtained with the static probe at $\theta = \pm 75^{\circ}$. Agreement is very good for Ω = +712 rpm, and within the scatter for Ω = -1284 rpm.

The shrouds appear to have produced the more gradual pressure gradient desired. The repeatability evidenced in the photographic data appears to confirm that gross unsteadiness in the flow due to vortex shedding has been surpressed.

There does appear to be some variation in the pressure distribution with rpm. Whether this change in pressure distribution itself can account for the shift in separation point with change in rotation speed, for which data was presented in Reference 1, will require further investigation. It should be remembered that the intent of this experimental program was not only to investigate the boundary layer velocity profile at separation for upstream and downstream motion of a separation point, but also to check the results of the theory of Reference 2 as regards the relative motion of the separation point itself with wall velocity variation for walls in motion downstream, and to obtain similar data for the upstream case where the analysis provided no quantitative estimates.

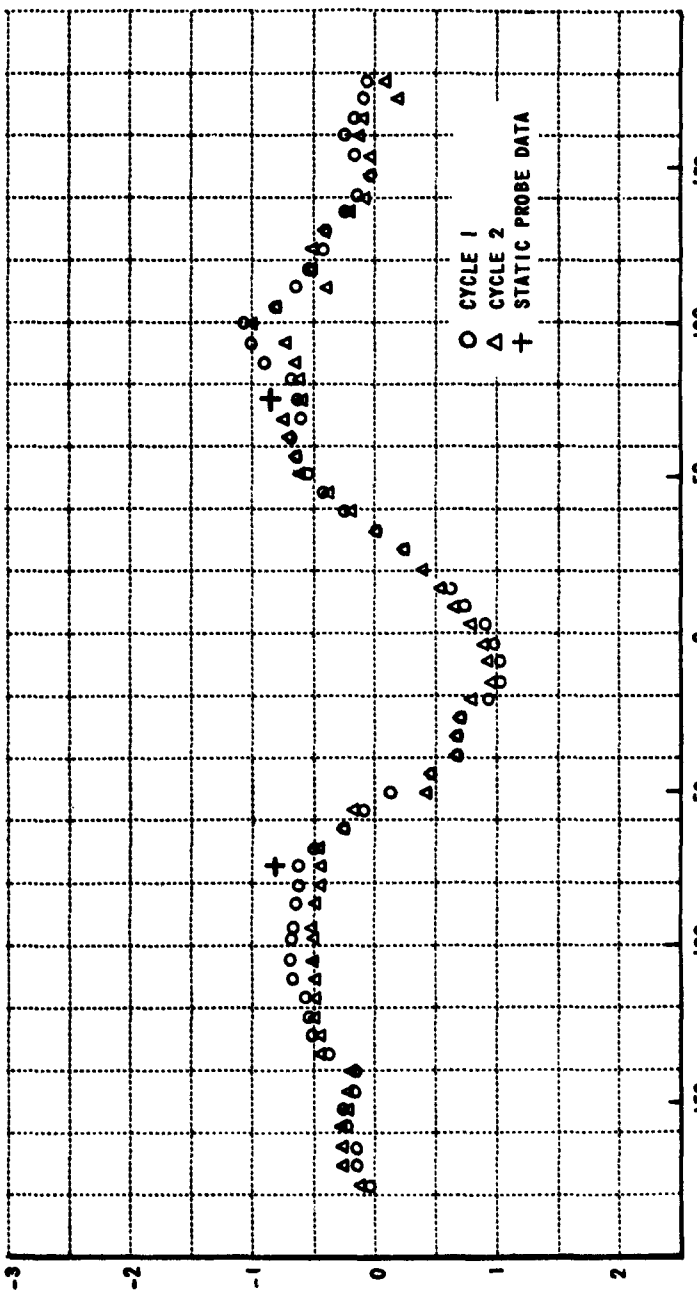

Figure 3 $\Delta p_s/q$ vs θ FOR SHROUDED ROTATING CYLINDER
$\Omega = -1284$ RPM $(Re)_D = 1.2 \times 10^5$

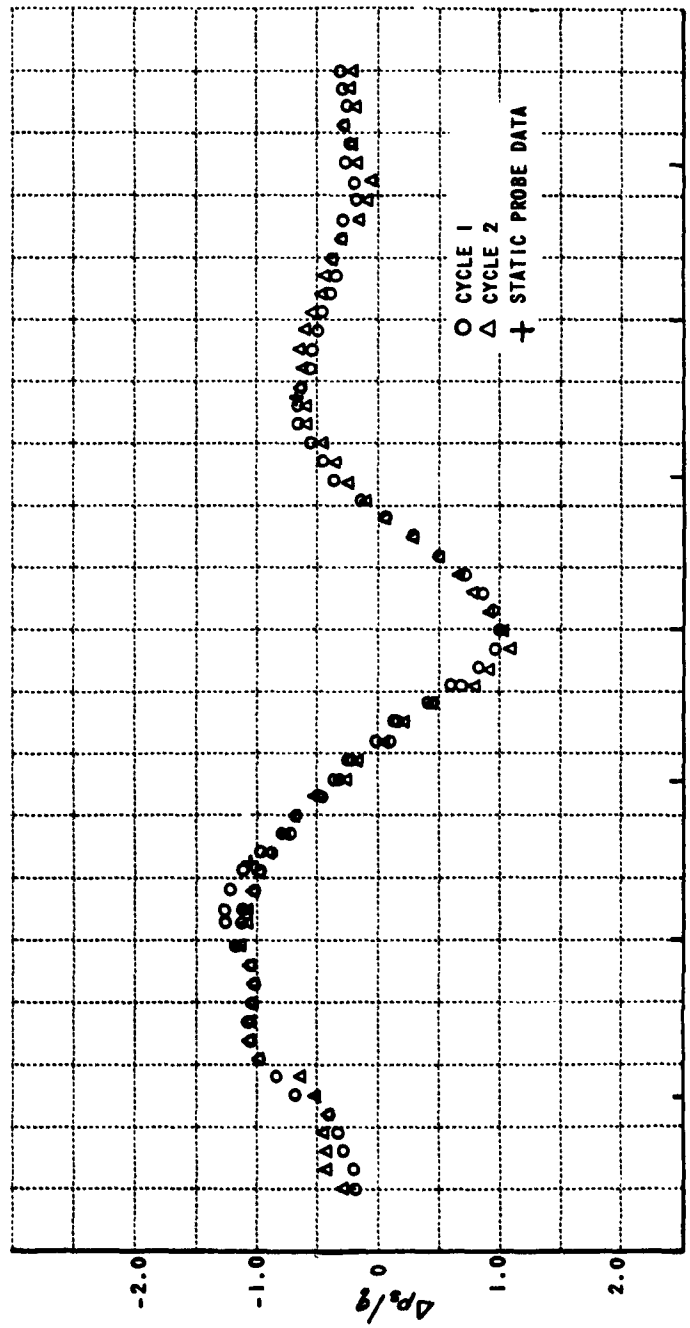

Figure 4 $\Delta p_s/q$ vs θ FOR SHROUDED ROTATING CYLINDER
Ω = 712 RPM $(Re)_D = 1.2 \times 10^5$

Velocity profiles have also been obtained for the outer portion of the boundary layer at $\theta = 90^{\circ}$ for a range of cylinder rotational speeds between $\Omega = 0$ and $\Omega = -1750$ rpm. This data is not presented here because it is incomplete; the probe cannot accurately measure the flow in the critical region of the boundary layer near the cylinder. For this region, hot-wire equipment must be used. However the total head probe data will be useful as a check on the hot-wire results and will be particularly useful in defining the outer edge of the boundary layer, where the total pressure approaches the constant value of the outer flow, regardless of the variation in velocity in the outer flow.

B. Theoretical Analyses

The initial theoretical effort during this program is concerned with a continuation of the work reported in Reference 4. This work was a study of possible disturbance patterns which may exist in the flow field produced by a single compressor stage — with a view to the description of possible three-dimensional or partial-span modes.

It should be made clear that this theoretical study is not directed toward attempts to predict specific characteristics of rotating stall phenomena, such as speed of propagation, number of stall zones, or the prediction of when rotating stall will occur in terms of compressor characteristics. Rather, the investigation is concerned with compatibility conditions in the flow which determine whether rotating stall is a permissible disturbance of the particular type of flow considered.

It was found in Reference 4 that, in a two-dimensional cascade, stall must propagate normal to the blade elements and cannot propagate in an oblique direction. For the single-stage axisymmetric case having a mean swirl of the free-vortex type, it was found that no partial-span disturbance of the rotating stall type was possible and, further, that only disturbances propagating with the blade rotation velocity were possible. These are potential

flow disturbances which are contingent on a combination of blade element negative lift-curve slope, and steady hysteresis of the lift curve.

Initial effort during the first quarter was devoted to an attempt to obtain solutions to the basic differential equations treated in Reference 4 in which the assumed mean flow included wheel-type swirl, rather than free-vortex-type swirl as treated in Reference 4. During the early stage of this work, the differential equations reported in Reference 4 were checked, and it was found that there was an error in one of the terms. It was felt that, because of this, there could be a change in the results of the free-vortex-type swirl analysis; therefore, the analysis was repeated based on the corrected equations.

Corrected Free-Vortex Swirl Analysis

The notation and coordinate systems used here are the same as those of Reference 4. Cylindrical coordinates (x , r , θ) are used with the x -axis centered in the compressor disc. The mean axial flow velocity component is U_0 , and there is, in addition, a mean tangential flow velocity $U_0 S(r)$. The compressor disc is represented by an axisymmetric actuator located at $x = 0$.

The general equations for the convection of vorticity (Eq. 27 of Reference 4) are:

$$\frac{\partial \underline{\omega}}{\partial t} + (\underline{q} \cdot \nabla)\underline{\omega} = (\underline{\omega} \cdot \nabla)\underline{q} \tag{1}$$

where $\underline{\omega}$ is the vorticity vector and $\underline{q}$ is the velocity vector. We write

$$\underline{q} \equiv U_0 + u, v, U_0 S(r) + w \tag{2}$$

$$\underline{\omega} \equiv \frac{U_0}{r}(rS)_r + \xi, \eta, \zeta \tag{3}$$

where (u , v , w) and (ξ , η , ζ) are perturbation components, and

$$\left.\begin{aligned} \xi &= \frac{1}{r}(rw)_r - \frac{1}{r} v_\theta \\ \eta &= \frac{1}{r} u_\theta - w_\theta \\ \zeta &= v_x - u_r \end{aligned}\right\} \tag{4}$$

from the relation

$$\underline{\Omega} = \nabla \times \underline{q}$$

Equation (1) becomes, after linearization,

$$\left(\frac{\partial}{\partial t} + U_0 \frac{\partial}{\partial x} + \frac{U_0 S}{r} \frac{\partial}{\partial \theta}\right) \begin{Bmatrix} \xi \\ \eta \\ \zeta \end{Bmatrix} \approx \begin{Bmatrix} -\left[\frac{U_0}{r}(rS)_r\right]_r + \frac{U_0}{r}(rS)_r u_x \\ \frac{U_0}{r}(rS)_r v_x \\ \frac{U_0}{r}(rS)_r w_x + \frac{U_0}{r}(rS)_r \eta - \underline{2\frac{U_0 S}{r}\eta} \end{Bmatrix} \tag{5}$$

which corresponds to Eq. (33) of Reference 4; the underlined term on the right-hand side in the equation for ζ is a correction. For vortex swirl, $S \equiv \frac{K}{r}$, K a constant, Eqs. (5) become

$$\left(\frac{\partial}{\partial t} + U_0 \frac{\partial}{\partial x} + \frac{U_0 K}{r^2} \frac{\partial}{\partial \theta}\right) \begin{Bmatrix} \xi \\ \eta \\ \zeta \end{Bmatrix} = \begin{Bmatrix} 0 \\ 0 \\ -2\frac{U_0 K}{r^2}\eta \end{Bmatrix} \tag{6}$$

which is the corrected form of Eqs. (35) of Reference 4. The solutions for ξ and η are

$$\begin{aligned} \xi &= f(\lambda, r) \\ \eta &= g(\lambda, r) \end{aligned} \tag{7}$$

as before (Eqs. (36), (37) and (40) of Reference 4) where

$$\lambda = \theta - \left(\omega + \frac{K}{r^2}\right) x + \omega U_0 t \tag{8}$$

However, we must replace Eq. (38) of Reference 4 for the ζ component of perturbed vorticity by the solution of

$$\left(\frac{\partial}{\partial t} + U_0 \frac{\partial}{\partial x} + \frac{U_0 K}{r^2} \frac{\partial}{\partial \theta}\right) \zeta = -\frac{2 U_0 K}{r^2} g(\lambda, r) \tag{9}$$

subject to

$$\zeta_+ - \frac{K}{r}\xi_+ = \frac{K}{r} f(\lambda_+, r) \tag{10}$$

The "+" subscript refers to conditions just downstream of the compressor disc, i.e., at $x = 0+$. A solution of Eq. (9) subject to Eq. (10) is

$$\zeta = \frac{K}{r} f(\lambda, r) - \frac{2Kx}{r^2} g(\lambda, r) \tag{11}$$

which replaces Eq. (38) of Reference 4.

Equation (43) of Reference 4 now becomes

$$-r\omega f_\lambda + (rg)_r - \frac{2Kx}{r^2} g_\lambda = 0 \tag{12}$$

which, at the actuator disc ($x = 0$) is

$$-\omega r f_{+\lambda} + (rg_+)_r = 0 \tag{13}$$

as before. The remainder of the analysis proceeds as before; the essential change in the results reported in Reference 4 for free-vortex swirl is the added second term on the right-hand side of Eq. (11), which disappears at the actuator disc and, hence, does not affect the succeeding analysis which is based on conditions at the disc.

Wheel-Type Swirl Analysis

For wheel-type swirl,

$$S(r) = Kr \tag{14}$$

and Eqs. (5) become

$$\left(\frac{\partial}{\partial t} + U_0 \frac{\partial}{\partial x} + KU_0 \frac{\partial}{\partial \theta}\right) \begin{Bmatrix} \xi \\ \eta \\ \zeta \end{Bmatrix} = 2KU_0 \frac{\partial}{\partial x} \begin{Bmatrix} u \\ v \\ w \end{Bmatrix} \tag{15}$$

Equations (15) plus Eq. (4) relating (ξ , η , ζ) to (u , v , w) constitute the six simultaneous differential equations relating the three perturbation vorticity components and the three perturbation velocity components for wheel-type swirl.

If the independent variables are transformed as

$$x' = \frac{x}{R_o} \quad , \quad r' = \frac{r}{R_o} \quad , \quad \tau = \frac{U_o t}{R_o}$$

and if

$$u = U_o u'$$

$$v = U_o v'$$

$$w = U_o w' ,$$

on substituting Eq. (4) in Eqs. (15), we obtain

$$\begin{aligned} \frac{D}{D\tau}\left[\frac{\partial}{\partial r'}(r'w') - \frac{\partial v'}{\partial \theta}\right] &= 2Kr'\frac{\partial u'}{\partial x'} \\ \frac{D}{D\tau}\left[\frac{\partial}{\partial x'}(r'w') - \frac{\partial u'}{\partial \theta}\right] &= 2Kr'\frac{\partial v'}{\partial x'} \\ \frac{D}{D\tau}\left[\frac{\partial u'}{\partial r'} - \frac{\partial v'}{\partial x'}\right] &= 2Kr'\frac{\partial w'}{\partial x'} \end{aligned} \tag{16}$$

where

$$\frac{D}{D\tau} \equiv \frac{\partial}{\partial \tau} + \frac{\partial}{\partial x'} + K\frac{\partial}{\partial \theta}$$

It is possible to derive from Eq. (16) partial differential equations, each in terms of u' , v' and w' only, but of higher order. That for u' is

$$\begin{aligned} &\frac{D}{D\tau}\left\{\frac{\partial}{\partial r'}\left[r'\frac{\partial^2 u'}{\partial r' \partial \theta} + \frac{r'(r'+1)}{r'-1}\frac{\partial^3 u'}{\partial x'^2 \partial \theta}\right]\right\} \\ &-4K\frac{\partial}{\partial r'}\left[\frac{(r')^3}{r'-1}\frac{\partial^2 u'}{\partial x'^2}\right] = 0 \end{aligned} \tag{17}$$

and that for v' is

$$\frac{D}{D\tau}\left\{\frac{2r'}{r'+1}\frac{\partial^4(r'v')}{\partial x'^3\partial r'}+\frac{1-r'}{r'(r'+1)}\frac{\partial^4(r'v')}{\partial x'\partial r'\partial\theta^2}\right\}-2K\frac{\partial^4(r'v')}{\partial x'^3\partial\theta}=0 \tag{18}$$

None of the sets of equations, (4) and (15), (16), or (17) and (18), have as yet been solved, nor does it appear that solutions will be obtainable without simplifications.

Analysis for Mean Flow with Swirl Through a Narrow Annulus

If it is assumed in Eq. (5) that $S = K$ (a constant), $v = 0$ and that u and w do not vary with r, then the flow could be considered as approximately that through a very narrow annulus. If this annulus is centered at R_o, Eqs. (5) can be written

$$\left(\frac{\partial}{\partial t}+U_o\frac{\partial}{\partial x}+\frac{U_oK}{R_o}\frac{\partial}{\partial\theta}\right)\begin{Bmatrix}\xi\\ \eta\\ \zeta\end{Bmatrix}=\frac{KU_o}{R_o}\begin{Bmatrix}\frac{\partial u}{\partial x}\\ 0\\ \frac{\partial w}{\partial x}-\eta\end{Bmatrix} \tag{19}$$

As from Eq. (4)

$$\left.\begin{aligned}\xi&=\frac{\partial w}{\partial v}-\frac{1}{R_o}\frac{\partial v}{\partial\theta}=0\\ \eta&=\frac{1}{R_o}\frac{\partial u}{\partial\theta}-\frac{\partial w}{\partial x}\\ \zeta&=\frac{\partial v}{\partial x}-\frac{\partial u}{\partial r}\quad=0\end{aligned}\right\} \tag{20}$$

we have from Eq. (19),

$$\frac{\partial u}{\partial x}=0\,,\qquad \frac{\partial w}{\partial x}-\eta=0 \tag{21}$$

or

$$u=u(\theta,t) \tag{22}$$

and from Eqs. (20) and (21)

$$\frac{\partial w}{\partial x} = \frac{1}{2R_o}\frac{\partial u}{\partial \theta} \tag{23}$$

The continuity equation is

$$\frac{\partial u}{\partial x} + \frac{1}{R_o}\frac{\partial w}{\partial \theta} = 0 \tag{24}$$

from which, as $\frac{\partial u}{\partial x} = 0$,

$$\frac{\partial w}{\partial \theta} = 0$$

or

$$w = w(x,t) \tag{25}$$

From Eq. (19)

$$\frac{\partial \eta}{\partial t} + U_o\frac{\partial \eta}{\partial x} + \frac{U_o K}{R_o}\frac{\partial \eta}{\partial \theta} = 0$$

so that

$$\eta = g(\lambda),$$

where

$$\lambda = \theta - \left(a + \frac{K}{R_o}\right)x + a U_o t \tag{26}$$

As in Reference 4, γ is defined as the circulation per unit angle on the actuator disc. For a specific blade element (Eq. 45 of Reference 4)

$$\frac{\partial \gamma}{\partial t} + kU_o\frac{\partial \gamma}{\partial \theta} = U_o R_o q_+ \tag{27}$$

where kU_o is the rotational velocity of the blade elements.

Let

$$\gamma(\theta,t) = \gamma'(\lambda_+, \sigma)$$

where

$$\lambda_+ = \theta + a U_o t$$
$$\sigma = \theta - kU_o t$$

Under this transformation, which is permissible except for $\alpha = -k$, Eq. (27) becomes

$$\frac{\partial \gamma'}{\partial \lambda_+} = \frac{R_0}{\alpha + k} g(\lambda_+) \tag{28}$$

which can be integrated to give

$$\gamma' = \frac{R_0}{\alpha + k} \int_0^{\lambda_t} g(\tau)\, d\tau + m(\sigma) \tag{29}$$

We have from Eq. (25) that $w = w(x,t)$ and from Eq. (21) that $\eta = \frac{\partial w}{\partial x}$, or that

$$\eta = g(\lambda) = \frac{\partial w(x,t)}{\partial x} \tag{30}$$

Here, g can at most be a constant, say, g_0. From Eqs. (23) and (30)

$$\frac{\partial u}{\partial \theta} = 2R_0 g_0$$

hence,

$$u = 2R_0 g_0 \theta + f(t)$$

However, as $u(\theta,t) = u(\theta + 2\pi, t)$, g_0 must be zero.

Thus,

$$\gamma' = m(\sigma) = m(\theta - k U_0 t)$$

and the only circulation disturbance of the rotating stall type possible is one fixed in the blades.

IV WORK FOR THE NEXT QUARTER

Experimental Program

Work will continue with the rotating cylinder to obtain boundary layer velocity profiles at separation for the wall moving both downstream and upstream. The development of the boundary layer velocity profile as the separation point is approached will also be investigated. Hot-wire anemometer equipment will be available for this work.

Theoretical Program

Work will continue on the compatibility conditions relating disturbances in circulation in the actuator disc to the appearance of vorticity downstream. Initially, the narrow annulus configuration will be emphasized; attempts will be made to relax the assumptions made thus far ($v = 0$, no variation of u and w with radius) which are undoubtedly oversimplified.

V REFERENCES

1. Vidal, R. J. Research on Rotating Stall in Axial Flow Compressors Part III - Experiments on Laminar Separation From a Moving Wall WADC TR 59-75, Part III January 1959

2. Hartunian, R. A. and Moore, F. K. Research on Rotating Stall in Axial Flow Compressors Part II - On the Separation of the Unsteady Laminar Boundary Layer WADC TR 59-75, Part II January 1959

3. Wilder, J. G., Hindersinn, K. and Weatherston, R. Design of an Air Supply System and Test Section for Research on Scavenging Systems for Propulsion Wind Tunnels WADC TR 56-6 December 1955

4. Moore, F. K. Research on Rotating Stall in Axial Flow Compressors Part IV - A Preliminary Study of Three-Dimensional Rotating Stall WADC TR 59-75, Part IV January 1959

DISTRIBUTION

			No. of Copies
U. S. Army Materiel Command Harry Diamond Laboratories Washington 25, D. C.			
ATTN:	R. D. Hatcher	Lab 300	1
	J. Kirshner	Br. 310	1
	K. Scudder	310	3
	R. Warren	310	1
	K. Woodward	310	1
	A. Talkin	310	1
	S. Katz	310	1
	Library	010	5
	Technical Information Office	012	2
	Contracts	090	1
Commander Aeronautical Systems Division Wright-Patterson Air Force Base, Ohio			
ATTN:	ASRMPT-1		10
ATTN:	ASRNGC-1/SAY		1
Commander Armed Services Technical Information Agency Arlington Hall Station Arlington 12, Virginia			
ATTN:	T1PDR		10
Cornell Aeronautical Laboratory, Inc. Buffalo 21, New York			10